Acta Pharm. **73** (2023) 269–280
https://doi.org/10.2478/acph-2023-0015

Original research paper

Rosavin exerts an antitumor role and inactivates the MAPK/ERK pathway in small-cell lung carcinoma *in vitro*

RUI LIU[a]
CUIHONG JIANG[a]
ZHIZHENG ZHAO
YUTONG LV
GAOXING WANG*

Department of Oncology, Guang'anmen Hospital, China Academy of Chinese Medical Sciences (South Campus) Beijing 102618, China

Accepted December 3, 2022
Published online December 3, 2022

ABSTRACT

This study attempts to explore the function and mechanism of action of rosavin in small-cell lung cancer (SCLC) *in vitro*. The viability and clone formation of SCLC cells were assessed using cell counting kit-8 and colony formation assays, respectively. Apoptosis and cell cycle were detected using flow cytometry and cell cycle analysis, respectively. Wound healing and transwell assays were performed to evaluate the migration and invasion of SCLC cells. Besides, protein levels of p-ERK, ERK, p-MEK and MEK were determined using Western blot analysis. Rosavin repressed the viability and clone formation of SCLC cells, and promoted apoptosis and G_0/G_1 arrest of SCLC cells. At the same time, rosavin suppressed migration and invasion of SCLC cells. Moreover, protein levels of p-ERK/ERK and p-MEK/MEK were decreased after rosavin addition in SCLC cells. Rosavin impaired malignant behaviors of SCLC cells, which may be associated with inhibition of the MAPK/ERK pathway *in vitro*.

Keywords: small-cell lung cancer, rosavin, MEK, ERK

Lung cancer is a serious threat to public health with high morbidity and mortality in the world (1, 2). It is estimated that about 2.1 million new cases of lung cancer are diagnosed in 2018 (3, 4). Based on histological categories, lung cancer is classified as small-cell lung cancer (SCLC) and non-small-cell lung cancer (NSCLC) (5, 6). SCLC accounts for about 15 % of lung cancer, which is featured by a rapid proliferation rate and early metastases (7, 8). Currently, chemotherapy and radiotherapy are the mainstays of SCLC therapy (9, 10). However, there is still a dismal prognosis for SCLC patients at present (11–13). Therefore, it is important to seek novel effective tactics for SCLC treatment.

[a] These two authors contributed equally to this study.
* Correspondence; email: drruiliu@163.com

Rosavin refers to an alkylbenzene diglycoside compound, which is a vital active ingredient of *Rhodiola rosea* L. (14). It is proven that rosavin possesses anticancer and antioxidative efficacy (15–17). Indeed, convincing evidence has demonstrated the important function of rosavin in several diseases (18, 19). For instance, rosavin is demonstrated to alleviate ovariectomy-caused osteoporosis in mice (18). Rosavin is demonstrated to inhibit inflammation and pulmonary fibrosis induced by bleomycin in mice (19). Nevertheless, few reports have illustrated the biological role of rosavin in SCLC.

It is reported that activation of the MAPK/ERK pathway is closely associated with the development of many cancers (20–22) including SCLC (23). For example, activation of the MAPK/ERK pathway contributes to the survival of SCLC cells (24). Suppression of the MAPK/ERK pathway can block many mechanisms promoting metastasis of SCLC cells (25). Notably, a study from Marchev *et al.* has indicated that rosavin can affect the apoptosis of T cells *via* regulating the MAPK/ERK pathway, suggesting its potential in the regulation of immune diseases and cancers (26). However, whether rosavin makes an impact on SCLC development *via* regulating the MAPK/ERK pathway remains unclear.

In this study, we explored the specific influences of rosavin on SCLC cells as well as underlying mechanisms implicated in these processes *in vitro*.

EXPERIMENTAL

Chemical reagent

Rosavin is also termed (*E*)-3-phenyl-2-propenyl 6-*O*-α-L-arabinopyranosyl-β-D-glucopyranoside, which is isolated from the root of *Rhodiola rosea* L. Its chemical structure is shown in supplement. It is a yellow paste and is soluble in methanol, ethanol, DMSO and other organic solvents. Rosavin (purity ≥ 98 %) stock solutions dissolved in DMSO were obtained from Nuodande Standard Technical Services (China). The concentration of rosavin stock solutions was 1.0 mg mL^{-1}, and rosavin working solutions were prepared by serial dilution of the stock solutions with methanol (Sigma Aldrich, China).

Cell culture and treatment

Human SCLC cell lines (H69, H446 and H526) were purchased from the American Type Culture Collection (USA). All cells were cultured in Roswell Park Memorial Institute (RPMI) 1640 medium (Thermo Fisher Scientific, USA) containing 10 % fetal bovine serum (FBS; Gibco, USA) and 1 % penicillin/streptomycin (Gibco). Under a condition of 95 % humidity, 5 % CO_2 and 37 °C, these cells were incubated.

To explore the role of rosavin in SCLC cells, H69, H526 and H446 cells were added into 96-well plates and were cultured to 70–80 % confluent. Then these cells were exposed to different concentrations of rosavin (0, 5, 10, 20, 50 and 100 μmol L^{-1}) for 72 h at 37 °C.

Cell counting kit (CCK)-8 assay

The viability of H69, H526 and H446 cells was assessed according to instructions of a Cell Counting Kit-8 (Beyotime, Shanghai, China). In brief, cells (1×10^3 cells/well) were

plated into 96-well plates, followed by incubation for 24, 48 and 72 h. Then CCK-8 solution (10 μL) was added to react for 2 h. The optical density of each well was measured at 490 nm using a microplate reader (MG LABTECH, USA).

Colony formation assay

H69, H526 and H446 cells were digested and then put into six-well plates at a density of 1×10^3 cells/well. After these cells were incubated at 37 °C for 2 weeks, cells were washed twice with phosphate-buffered saline (PBS), fixed with methanol for 20 min, and stained with 0.5 % crystal violet solution for another 20 min at room temperature. At last, a Nikon microscope was used to count the colony number in five randomly chosen fields.

Flow cytometry

H69, H526 and H446 cells were digested through trypsin without EDTA, and the cell suspension was centrifuged at 1,000 × g for 5 min at room temperature. Then these cells were washed with PBS twice and were centrifuged at 1,000 × g for 5 min at room temperature. The supernatant was discarded and cells were re-suspended in 1 × binding buffer. Afterwards, re-suspended cells were incubated with 5 μL propidium iodide staining solution (Beyotime) and 5 μL Annexin V-FITC solution (Beyotime) in the dark at room temperature for 15 min. The percentage of cell apoptosis was evaluated *via* a FACSCalibur Flow Cytometer (Becton Dickinson, USA).

Cell cycle analysis

H69, H526 and H446 cells were dissociated *via* trypsin without EDTA, and the cell suspension was centrifuged at 1,000 × g for 5 min at room temperature. Then cells were washed using PBS twice and were again centrifuged at 1,000 × g for 5 min at room temperature. After the supernatant was discarded, cells were re-suspended and fixed in 70 % (*V*/*V*) ethanol at 4 °C for 2 h. Ethanol used was discarded via centrifugation at 1,000 × g for 5 min at 4 °C. After being washed with PBS twice, cells were incubated with 400 μL propidium iodide staining solution in the dark for 20 min. Then cell samples were subjected to a FACSCalibur Flow Cytometer.

Wound healing assay

H69, H526 and H446 cells (5×10^4 cells/well) were plated into 6-well plates, which were then cultured in RPMI 1640 medium containing 10 % FBS. When the cell monolayer was formed, scratches were made and the relative length of scratches was recorded. After being washed via PBS, cells were cultured in an FBS-free medium for 24 h. Then cells were observed using an inverted microscope (Nikon, Japan) to gauge the wound-healing distance. The following formula was used to calculate the wound healing rate: (1–24 h scratch width/0 h scratch width) × 100.

Transwell assay

The invasion ability of H69, H526 and H446 cells was assessed through transwell assays. Transwell chambers (8-mm pore size; Corning, USA) coated with Matrigel (BD

Biosciences, USA) were used. Cell suspension (100 μL) suspended in an FBS-free medium was loaded into upper chambers. Also, a culture medium (600 μL) containing 10 % FBS was appended to the lower chambers. After the chambers were incubated for 24 h, a cotton swab was used to wipe off residual cells on the upper surface of the inner chamber. Meantime, cells in the lower surface of chambers were fixed using paraformaldehyde and dyed using crystal violet. Invasive cells were counted under an optical microscope.

Western blot analysis

Proteins were extracted from H69, H526 and H446 cells via RIPA buffer (Beyotime). Then lysates were centrifuged at 12, 000 r/min for 10 min at 4 °C, and cell supernatant was mixed with 5 × loading buffer and denatured at 100 °C for 5 min. Next, the concentration of isolated proteins was examined using a BCA kit. The sodium dodecyl sulphate-polyacrylamide gels with 10 % separation gel and 5 % stacking gel were prepared. The protein samples (10 μL) were separated by electrophoresis in 1 × buffer (9.4 g glycine, 1.51 g Tris-base, 0.5 g SDS, 500 mL ddH_2O) at 80 V for 30 min and at 120 V for 1 h, and were moved to polyvinylidene difluoride membranes. After being blocked with skim milk, primary antibodies (Abcam, USA) against ERK (1:1000, ab17942), p-ERK (1:1000, ab201015), MEK (1:20000, ab178876), p-MEK (1:1000, ab278564) and β-actin (1:200, ab115777) were added to incubate overnight. Subsequently, the secondary antibody (1:2000, ab6721) was added to incubate for 1 h. Finally, blot detection was performed via a Bioimaging system (Bio-Rad, USA), and protein quantification was performed using Image J software (NIH, USA).

Statistical analysis

GraphPad Prism 7.0 (GraphPad Software Inc., USA) was used for performing statistical analysis. All experimental data were presented as mean ± standard deviation. Difference comparisons between two groups of data were performed using Student's *t*-test. Difference comparisons among multiple groups of data were performed using One-way ANOVA, accompanied by Tukey's test. $p < 0.05$ was regarded as statistical significance.

RESULTS AND DISCUSSION

Rosavin represses the viability and clone formation of SCLC cells

Firstly, the effect of rosavin on the proliferation of SCLC cells was determined by performing CCK-8 and colony formation assays. It came out that the viability of H69, H526 and H446 cells was attenuated by the addition of 5, 10, 20 and 50 μmol L^{-1} rosavin in a dose-dependent manner (Fig. 1a–c, $p < 0.05$). When 100 μmol L^{-1} rosavin was added, the ceiling effect was observed. Likewise, the addition of 5, 10, 20 and 50 μmol L^{-1} rosavin resulted in decreasing colony formation of H69, H526 and H446 cells in a dose-dependent manner compared to no rosavin (Fig. 1d–f, $p < 0.05$). When 100 μmol L^{-1} rosavin was added, the ceiling effect was observed.

Rosavin facilitates the apoptosis of SCLC cells

The result of flow cytometry analysis demonstrated that the percentage of apoptotic H69, H526 and H446 cells was elevated after the addition of 5, 10, 20 and 50 μmol L^{-1}

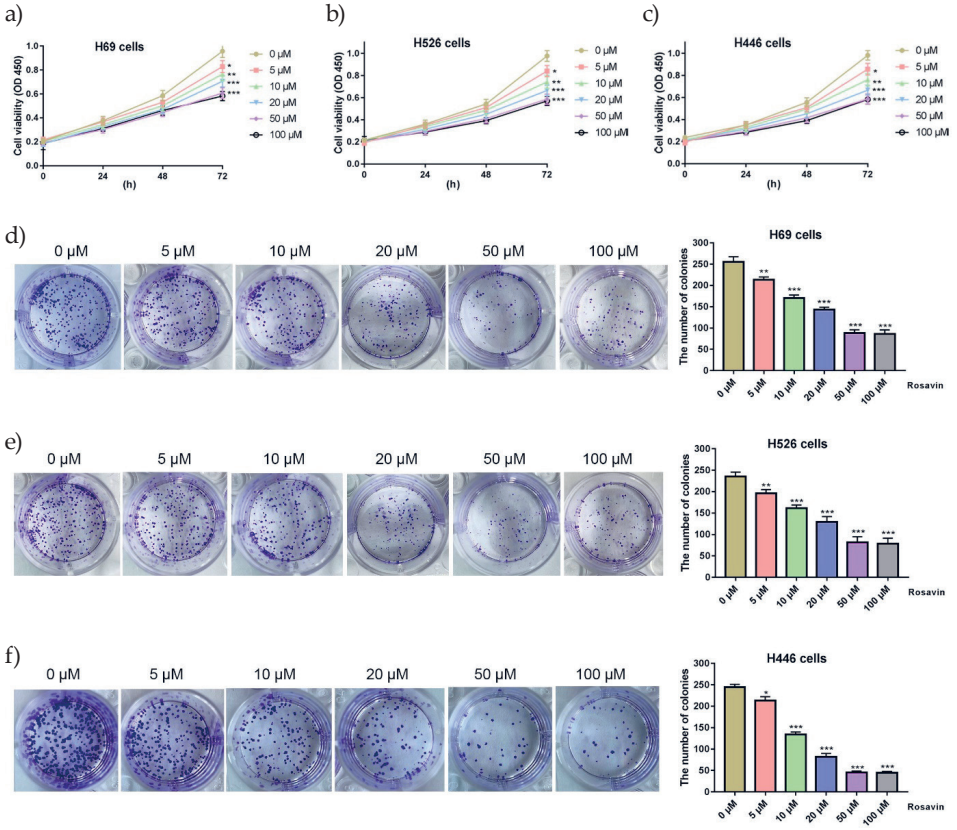

Fig. 1. Rosavin represses the viability and clone formation of SCLC cells. a–c) The viability of H69, H526 and H446 cells was evaluated by CCK-8 assay; d–f) The clone formation of H69, H526 and H446 cells was determined by colony formation assay. $^{*}p < 0.05$, $^{**}p < 0.01$, $^{***}p < 0.001$, *vs.* 0 μmol L^{-1} rosavin. Each experiment was performed in triplicate in three independent experiments ($n = 3$).

rosavin in a dose-dependent manner (Fig. 2a–c, $p < 0.01$). Also, when 100 μmol L^{-1} rosavin was added, the ceiling effect was observed.

Rosavin promotes G_0/G_1 arrest of SCLC cells

Likewise, the addition of 5, 10, 20, 50 and 100 μmol L^{-1} rosavin led to evident G_0/G_1 arrest of H69, H526 and H446 cells in comparison with no rosavin added (Fig. 3a–c).

Rosavin attenuates the migration and invasion abilities of SCLC cells while suppressing the MAPK/ERK pathway in SCLC cells

Additionally, wound healing and transwell assays were performed to detect the impacts of rosavin on migration and invasion in H69, H526 and H446 cells. As illustrated in Fig. 4a–c, rosavin (5, 10, 20 and 50 μmol L^{-1}) stimulation could distinctly reduce the wound healing rate

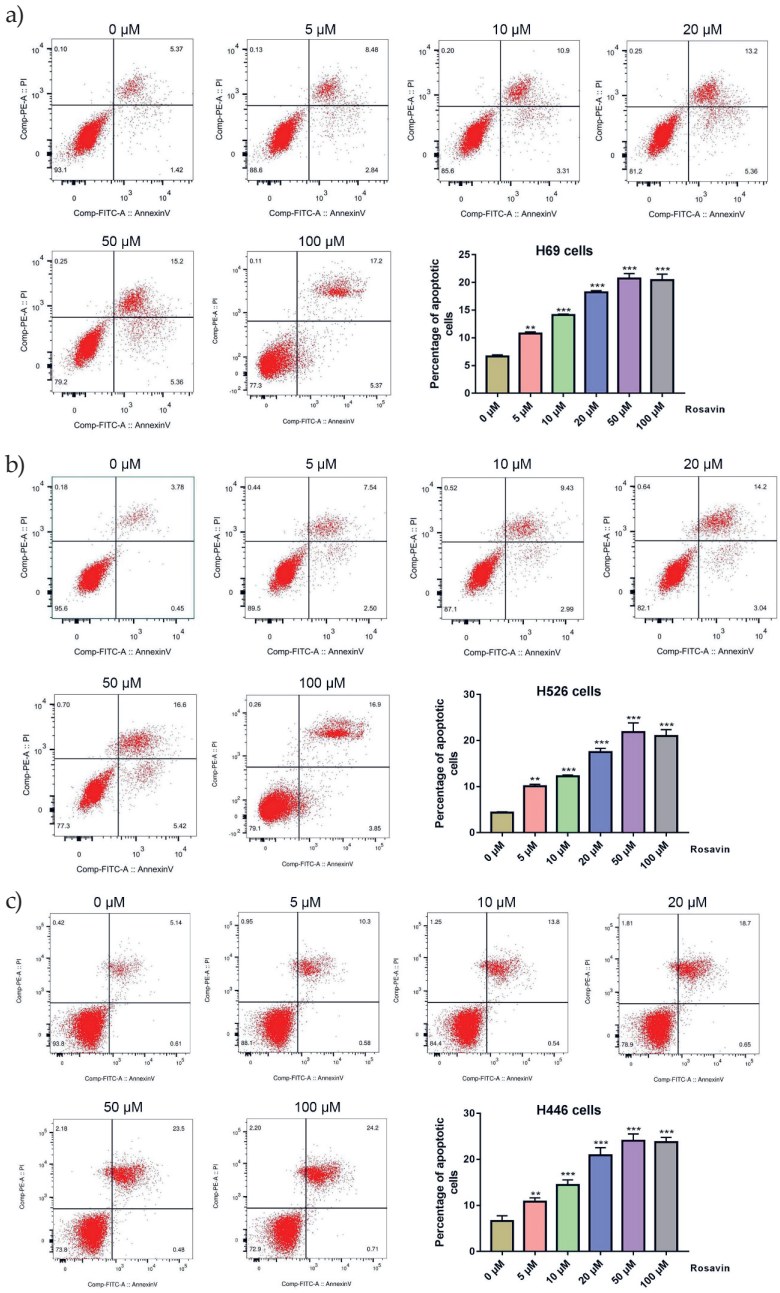

Fig. 2. Rosavin facilitates apoptosis of SCLC cells. a–c) The percentage of apoptotic H69, H526 and H446 cells was detected via flow cytometry. ***$p < 0.001$, *vs.* 0 μmol L^{-1} rosavin. Each experiment was performed in triplicate in three independent experiments ($n = 3$).

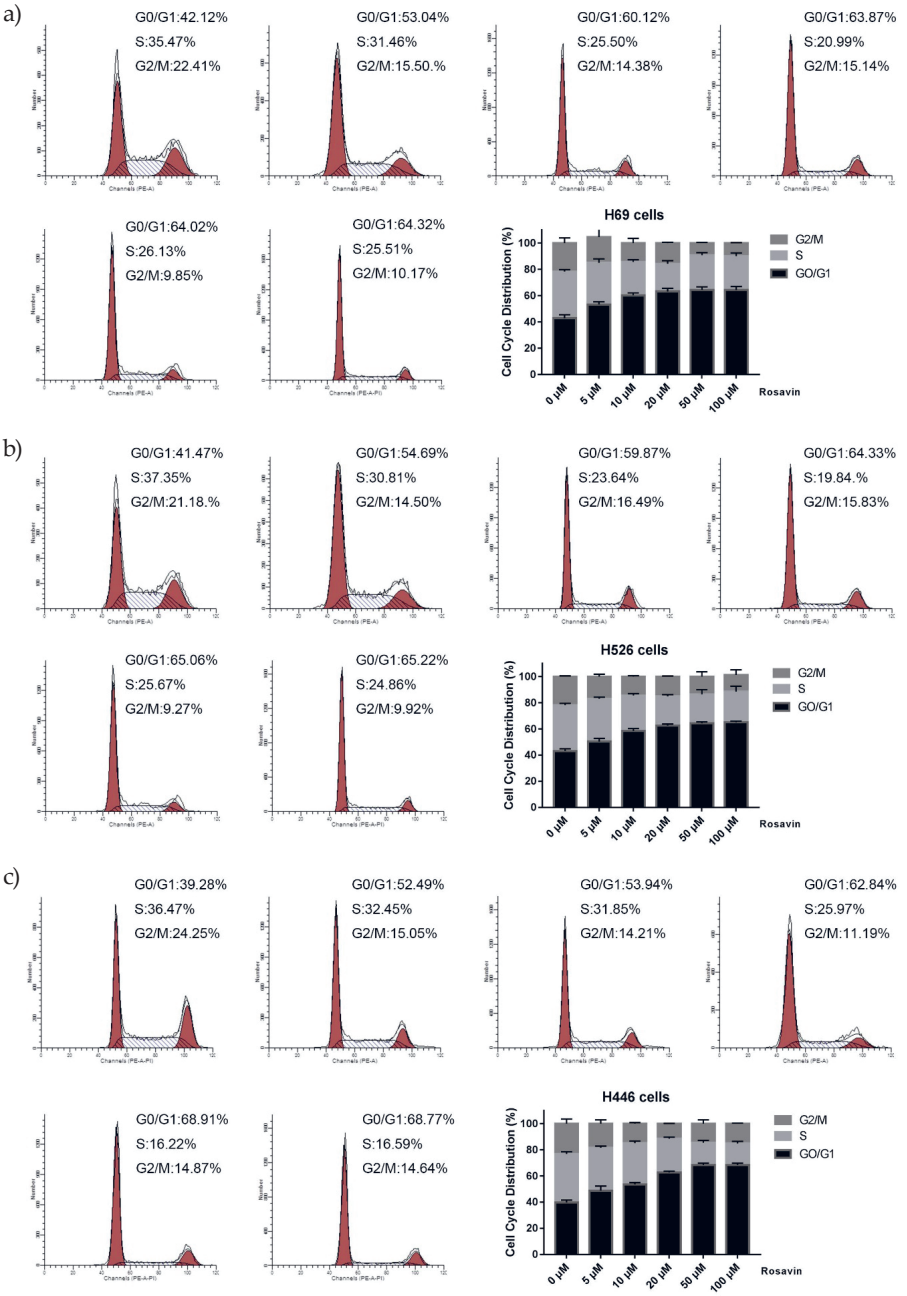

Fig. 3. Rosavin promotes G_0/G_1 arrest of SCLC cells. a–c) The cell cycle of H69, H526 and H446 cells was determined using cell cycle analysis, *vs.* 0 μmol L^{-1} rosavin. Each experiment was performed in triplicate in three independent experiments (n = 3).

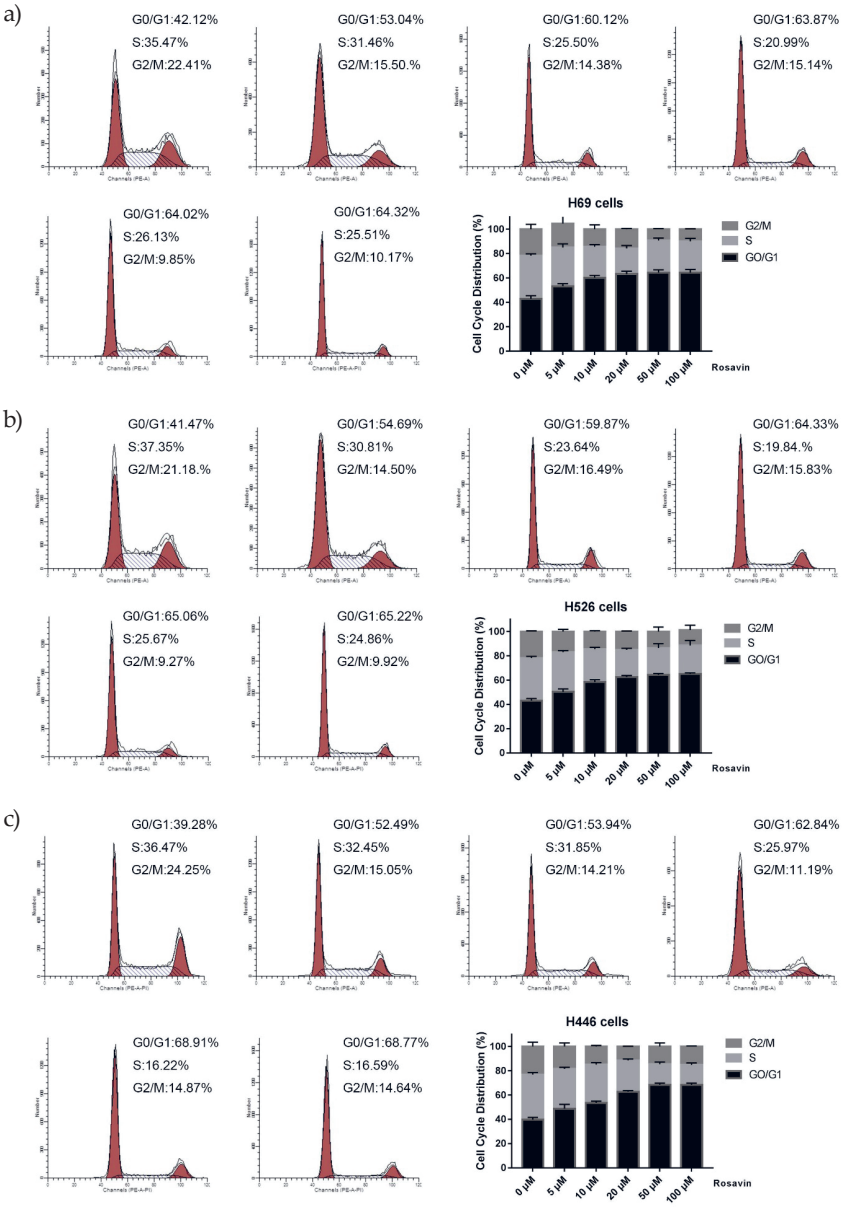

Fig. 4. Rosavin attenuates the migratory and invasive abilities of SCLC cells, and suppresses the MAPK/ERK pathway in SCLC cells. a–c) The migration of H69, H526 and H446 cells was detected by wound healing assay; d–f) the invasion of H69, H526 and H446 cells were detected by transwell assay; g–i) protein levels of p-ERK, ERK, p-MEK and MEK were detected by Western blot in H69, H526 and H446 cells. *$p < 0.05$, **$p < 0.01$, ***$p < 0.001$, *vs*. 0 μmol L^{-1} rosavin. Each experiment was performed in triplicate in three independent experiments ($n = 3$).

of H69, H526 and H446 cells in a dose-dependent manner compared to rosavin (0 μmol L^{-1}) stimulation ($p < 0.05$). The ceiling effect was observed when 100 μmol L^{-1} rosavin was added. Moreover, rosavin (5, 10, 20 and 50 μmol L^{-1}) stimulation reduced the numbers of invaded H69, H526 and H446 cells in a dose-dependent manner compared to rosavin (0 μmol L^{-1}) stimulation (Fig. 4d–f, $p < 0.001$). The ceiling effect was found when 100 μmol L^{-1} rosavin was added.

Finally, whether rosavin could affect the MAPK/ERK pathway was verified *via* the determination of pathway-related proteins (p-ERK, ERK, p-MEK and MEK). It was found that protein levels of p-ERK/ERK and p-MEK/MEK in H69, H526 and H446 cells were reduced by rosavin (5, 10, 20 and 50 μmol L^{-1}) addition in a dose-dependent manner (Fig. 4g–i, $p < 0.05$). Also, the ceiling effect was found when 100 μmol L^{-1} rosavin was added.

These outcomes consistently indicated that the MAPK/ERK pathway was inactivated by rosavin in SCLC cells.

Targeted therapy and immunotherapy have offered a promising direction for the precision treatment of lung cancer (27, 28). It is noted that rosavin is uncovered to play important roles in several pre-clinical models, such as inflammatory and diabetic models (29, 30). More importantly, the antitumor role of rosavin in bladder cancer and Ehrlich's tumor has been demonstrated (17, 31). In this context, we explored whether rosavin had an antitumor role in SCLC *in vitro*. We found that the addition of 5, 10, 20, 50 and 100 μmol L^{-1} rosavin repressed the viability, clone formation, migration and invasion of SCLC cells. However, the ceiling effect was observed when 100 μmol L^{-1} rosavin was added, suggesting that 50 μmol L^{-1} rosavin displayed the best antitumor role among these concentrations. At the same time, we found that rosavin facilitated apoptosis and G0/G1 arrest of SCLC cells. Our findings were similar to prior studies. For instance, extract from *Rhodiola rosea* rhizomes is previously reported to promote apoptosis and cell cycle arrest in neutrophil promyelophils (32, 33). Rosavin proved to impair the growth of malignant tumor cells in the liver (15). Altogether, the above outcomes suggest that rosavin prevented SCLC development *in vitro*, which highlighted a theoretical basis for further application of rosavin in SCLC therapy.

According to previous reports, the MAPK/ERK pathway is involved in SCLC development. For instance, activation of the MAPK/ERK pathway promotes the survival of SCLC cells (24). Several mechanisms facilitating metastasis of SCLC cells are inhibited after the inactivation of the MAPK/ERK pathway (25). Therefore, we performed Western blotting to explore whether rosavin could make an impact on the MAPK/ERK pathway in SCLC. We discovered that relative protein expression of p-ERK/ERK and p-MEK/MEK was decreased by rosavin addition in SCLC cells, implying that rosavin may repress SCLC development via inactivating the MAPK/ERK pathway. And rosavin-induced suppression of the MAPK/ERK pathway in SCLC was similar to the results of previous studies. Previously, rosavin is demonstrated to block the MAPK/ERK signalling pathway to impair the development of osteoclastogenesis (34). Rosavin is demonstrated to repress the MAPK/ERK pathway in L-glutamate-induced neurotoxicity (26). Taken together, these findings supported the conclusion that the suppressive influence of rosavin on SCLC development may be associated with the suppression of the MAPK/ERK pathway.

CONCLUSIONS

To conclude, we demonstrated that rosavin was capable of inhibiting the progression and development of SCLC *in vitro*, and the underlying mechanism had a connection with

the MAPK/ERK pathway. This investigation may provide a promising antitumor agent for SCLC treatment.

Funding. – This study was supported by the National Natural Science Foundation of China (81703918).

Conflicts of interest. – None.

Author's contributions. – RL and CHJ wrote the manuscript; ZZZ and GXW collected the data; all authors analyzed the data. All authors read and approved the final manuscript.

REFERENCES

1. Y. Wang, S. Zou, Z. Zhao, P. Liu, C. Ke and S. Xu, New insights into small-cell lung cancer development and therapy, *Cell Biol. Int*. **44**(8) (2020) 1564–1576; https://doi.org/10.1002/cbin.11359
2. A. Pavan, I. Attili, G. Pasello, V. Guarneri, P. F. Conte and L. Bonanno, Immunotherapy in small-cell lung cancer: from molecular promises to clinical challenges, *J. Immunother. Cancer* **7**(1) (2019) Article ID 205 (13 pages); https://doi.org/10.1186/s40425-019-0690-1
3. F. Bray, J. Ferlay, I. Soerjomataram, R. L. Siegel, L. A. Torre and A. Jemal, Global cancer statistics 2018: GLOBOCAN estimates of incidence and mortality worldwide for 36 cancers in 185 countries, *C. A. Cancer J. Clin*. **68**(6) (2018) 394–424; https://doi.org/10.3322/caac.21492
4. H. Sung, J. Ferlay, R. L. Siegel, M. Laversanne, I. Soerjomataram, A. Jemal and F. Bray, Global Cancer Statistics 2020: GLOBOCAN estimates of incidence and mortality worldwide for 36 cancers in 185 countries, *C. A. Cancer J. Clin*. **71**(3) (2021) 209–249; https://doi.org/10.3322/caac.21660
5. P. Goldstraw, Updated staging system for lung cancer, *Surg. Oncol. Clin. N. Am*. **20**(4) (2011) 655–666; https://doi.org/10.1016/j.soc.2011.07.005
6. G. P. Kalemkerian, Small cell lung cancer, *Semin. Respir. Crit. Care Med*. **37**(5) (2016) 783–796; https://doi.org/10.1055/s-0036-1592116
7. E. B. Bernhardt and S. I. Jalal, Small cell lung cancer, *Cancer Treat. Res.* **170** (2016) 301–322; https://doi.org/10.1007/978-3-319-40389-2_14
8. G. P. Kalemkerian and B. J. Schneider, Advances in small cell lung cancer, *Hematol. Oncol. Clin. North Am*. **31**(1) (2017) 143–156; https://doi.org/10.1016/j.hoc.2016.08.005
9. S. Sundstrom, R. M. Bremnes, S. Kaasa, U. Aasebo, R. Hatlevoll, R. Dahle, N. Boye, M. Wang, T. Vigander, J. Vilsvik, E. Skovlund, E. Hannisdal, S. Aamdal and G. Norwegian, Lung cancer study: Cisplatin and etoposide regimen is superior to cyclophosphamide, epirubicin, and vincristine regimen in small-cell lung cancer: results from a randomized phase III trial with 5 years' follow-up, *J. Clin. Oncol*. **20**(24) (2002) 4665–4672; https://doi.org/10.1200/JCO.2002.12.111
10. M. Takada, M. Fukuoka, M. Kawahara, T. Sugiura, A. Yokoyama, S. Yokota, Y. Nishiwaki, K. Watanabe, K. Noda, T. Tamura, H. Fukuda and N. Saijo, Phase III study of concurrent versus sequential thoracic radiotherapy in combination with cisplatin and etoposide for limited-stage small-cell lung cancer: results of the Japan Clinical Oncology Group Study 9104, *J. Clin. Oncol*. **20**(14) (2002) 3054–3060; https://doi.org/10.1200/JCO.2002.12.071
11. R. L. Siegel, K. D. Miller, H. E. Fuchs and A. Jemal, Cancer statistics, 2021, *C. A. Cancer J. Clin*. **71**(1) (2021) 7–33; https://doi.org/10.3322/caac.21654
12. T. F. Mott, Lung cancer: Management, *F. P. Essent*. **464** (2018) 27–30.
13. G. S. Jones and D. R. Baldwin, Recent advances in the management of lung cancer, *Clin. Med. (Lond)*. **18**(Suppl 2) (2018) s41-s46; https://doi.org/10.7861/clinmedicine.18-2-s41
14. C. Ma, J. Tang, H. Wang, G. Tao, X. Gu and L. Hu, Preparative purification of salidroside from *Rhodiola rosea* by two-step adsorption chromatography on resins, *J. Sep. Sci*. **32**(2) (2009) 185–191; https://doi.org/10.1002/jssc.200800438

15. A. Kucinskaite, V. Briedis and A. Savickas, Experimental analysis of therapeutic properties of *Rhodiola rosea* L. and its possible application in medicine, *Medicina (Kaunas)* **40**(7) (2004) 614–619.
16. Y. Li, J. Wu, R. Shi, N. Li, Z. Xu and M. Sun, Antioxidative effects of *Rhodiola* genus: Phytochemistry and pharmacological mechanisms against the diseases, *Curr. Top. Med. Chem.* **17**(15) (2017) 1692–1708; https://doi.org/10.2174/1568026617666161116141334
17. S. N. Udintsev and V. P. Shakhov, Decrease in the growth rate of Ehrlich's tumor and Pliss' lymphosarcoma with partial hepatectomy, *Vopr. Onkol.* **35**(9) (1989) 1072–1075.
18. H. Zhang, C. Ding, Y. Li, C. Xing, S. Wang, Z. Yu, L. Chen, P. Li and M. Dai, Data mining-based study of collagen type III alpha 1 (COL3A1) prognostic value and immune exploration in pan-cancer, *Bioengineered* **12**(1) (2021) 3634–3646; https://doi.org/10.1080/21655979.2021.1949838
19. X. Xin, D. Yao, K. Zhang, S. Han, D. Liu, H. Wang, X. Liu, G. Li, J. Huang and J. Wang, Protective effects of rosavin on bleomycin-induced pulmonary fibrosis via suppressing fibrotic and inflammatory signaling pathways in mice, *Biomed. Pharmacother.* **115** (2019) Article ID 108870 (8 pages); https://doi.org/10.1016/j.biopha.2019.108870
20. W. X. Peng, J. G. Huang, L. Yang, A. H. Gong and Y. Y. Mo, Linc-RoR promotes MAPK/ERK signaling and confers estrogen-independent growth of breast cancer, *Mol. Cancer* **16**(1) (2017) Article ID 161 (11 pages); https://doi.org/10.1186/s12943-017-0727-3
21. M. Pashirzad, R. Khorasanian, M. M. Fard, M. H. Arjmand, H. Langari, M. Khazaei, S. Soleimanpour, M. Rezayi, G. A. Ferns, S. M. Hassanian and A. Avan, The therapeutic potential of MAPK/ERK inhibitors in the treatment of colorectal cancer, *Curr. Cancer Drug Targets* **21**(11) (2021) 932–943; https://doi.org/10.2174/1568009621666211103113339
22. B. Wang, X. X. Zhu, L. Y. Pan, H. F. Chen and X. Y. Shen, PP4C facilitates lung cancer proliferation and inhibits apoptosis via activating MAPK/ERK pathway, *Pathol. Res. Pract.* **216**(5) (2020) Article ID 152910; https://doi.org/10.1016/j.prp.2020.152910
23. Z. Wang, G. Kan, C. Sheng, C. Yao, Y. Mao and S. Chen, ARHGEF19 regulates MAPK/ERK signaling and promotes the progression of small cell lung cancer, *Biochem. Biophys. Res. Commun.* **533**(4) (2020) 792–799; https://doi.org/10.1016/j.bbrc.2020.09.085
24. Y. Liu, Z. Zhang, T. Song, F. Liang, M. Xie and H. Sheng, Resistance to BH3 mimetic S1 in SCLC cells that up-regulate and phosphorylate Bcl-2 through ERK1/2, *Br. J. Pharmacol.* **169**(7) (2013) 1612–1623; https://doi.org/10.1111/bph.12243
25. S. Cristea and J. Sage, Is the canonical RAF/MEK/ERK signaling pathway a therapeutic target in SCLC?, *J. Thorac. Oncol.* **11**(8) (2016) 1233–1241; https://doi.org/10.1016/j.jtho.2016.04.018
26. A. S. Marchev, P. Dimitrova, I. K. Koycheva and M. I. Georgiev, Altered expression of TRAIL on mouse T cells via ERK phosphorylation by *Rhodiola rosea* L. and its marker compounds, *Food Chem. Toxicol.* **108**(Pt B) (2017) 419–428; https://doi.org/10.1016/j.fct.2017.02.009
27. R. Ruiz-Cordero and W. P. Devine, Targeted therapy and checkpoint immunotherapy in lung cancer, *Surg. Pathol. Clin.* **13**(1) (2020) 17–33; https://doi.org/10.1016/j.path.2019.11.002
28. E. C. Naylor, J. K. Desani and P. K. Chung, Targeted therapy and immunotherapy for lung cancer, *Surg. Oncol. Clin. N. Am.* **25**(3) (2016) 601–609; https://doi.org/10.1016/j.soc.2016.02.011
29. R. M. Montiel-Ruiz, M. E. Gonzalez-Trujano and M. Deciga-Campos, Synergistic interactions between the antinociceptive effect of *Rhodiola rosea* extract and B vitamins in the mouse formalin test, *Phytomedicine* **20**(14) (2013) 1280–1287; https://doi.org/10.1016/j.phymed.2013.07.006
30. M. Deciga-Campos, M. E. Gonzalez-Trujano, R. Ventura-Martinez, R. M. Montiel-Ruiz, G. E. Angeles-Lopez and F. Brindis, Antihyperalgesic activity of *Rhodiola rosea* in a diabetic rat model, *Drug Dev. Res.* **77**(1) (2016) 29–36; https://doi.org/10.1002/ddr.21289
31. Z. Liu, X. Li, A. R. Simoneau, M. Jafari and X. Zi, *Rhodiola rosea* extracts and salidroside decrease the growth of bladder cancer cell lines via inhibition of the mTOR pathway and induction of autophagy, *Mol. Carcinog.* **51**(3) (2012) 257–267; https://doi.org/10.1002/mc.20780

32. A. Majewska, G. Hoser, M. Furmanowa, N. Urbanska, A. Pietrosiuk, A. Zobel and M. Kuras, Antiproliferative and antimitotic effect, S phase accumulation and induction of apoptosis and necrosis after treatment of extract from *Rhodiola rosea* rhizomes on HL-60 cells, *J. Ethnopharmacol*. **103**(1) (2006) 43–52; https://doi.org/10.1016/j.jep.2005.05.051
33. X. Hu, S. Lin, D. Yu, S. Qiu, X. Zhang and R. Mei, A preliminary study: the anti-proliferation effect of salidroside on different human cancer cell lines, *Cell Biol. Toxicol*. **26**(6) (2010) 499–507; https://doi.org/10.1007/s10565-010-9159-1
34. W. Zhang, W. Zhang, L. Huo, Y. Chai, Z. Liu, Z. Ren and C. Yu, Rosavin suppresses osteoclastogenesis in vivo and in vitro by blocking the nuclear factor kappa-light-chain-enhancer of activated B cells (NF-kappaB) and mitogen-activated protein kinase (MAPK) signaling pathways, *Ann. Transl. Med*. **9**(5) (2021) Article ID 383 (14 pages); https://doi.org/10.21037/atm-20-4255